Proceedings of the XVIII ECSMGE 2024
GEOTECHNICAL ENGINEERING CHALLENGES
TO MEET CURRENT AND EMERGING NEEDS OF SOCIETY

ISBN 978-1-032-54816-6
DOI 10.1201/9781003431749-197

ECSMGE 24
XVIII EUROPEAN CONFERENCE ON SOIL MECHANICS AND GEOTECHNICAL ENGINEERING

Appraisal of various measures for liquefaction flowslide mitigation in a mild sloping ground

Évaluation de diverses mesures d'atténuation des glissements de liquéfaction dans un terrain en pente douce

M.H. Fansuri*
Universitas Pertahanan Republik Indonesia (Unhan RI), Bogor, Indonesia

M. Chang, R.R. Rayhansyah, H.J. Lin
National Yunlin Univ. Sci. & Tech. (YunTech), Douliu, Taiwan, ROC

T.C. Upomo, R. Kusumawardani
Universitas Negeri Semarang (Unnes), Semarang, Indonesia

**hamzah.fansuri@idu.ac.id*

ABSTRACT: Liquefaction-induced flowslides would cause significant damages and casualties as the case of 2018.9.28 incidences of Palu, Sulawesi, Indonesia, where the flowslides occurred immediately after a severe earthquake and led to an extremely-long distance of sliding on mild sloping ground. The conditions that would favour soil liquefaction and the associated flowsliding hence become the focus of the incident. Another issue deserved further attention, however, would be strategy for preventing or mitigating the problem. In accordance, the aim of this study is to apprise the performance and effectiveness of various measures on the mitigation of soil liquefaction and flowsliding. The mitigation measures considered herein include: stone-column (SC), micro-pile (MP), densification (DS), encased stone column (ESC) soil grouting (GT), and groundwater lowering (GL), which are commonly adopted in engineering practice. The performance and effectiveness of the mitigation measures are assessed numerically in terms of their responses in the excess pore pressure generation in soil as well as the lateral deformation of soil deposit due to the excitation of seismic motion. Results generally indicate the SC, ESC, and DS options are more effective in prohibiting the generation of excess pore pressure, and hence in reducing soil liquefaction, than the other options. We also notice the MP, SC, and ESC options would be more effective in preventing the lateral deformation, and therefore in avoiding the flowslide or lateral spread in soil deposit.

RÉSUMÉ: Les glissements de terrain induits par la liquéfaction causeraient des dommages et des pertes importants, comme dans le cas des incidents du 28 septembre 2018 à Palu, Sulawesi, en Indonésie, où les glissements de terrain se sont produits immédiatement après un grave tremblement de terre et ont conduit à une distance de glissement extrêmement longue sur un terrain en pente douce. Les conditions qui favoriseraient la liquéfaction des sols et les glissements d'écoulement associés deviennent alors au centre de l'incident. Une autre question qui mériterait davantage d'attention serait celle de la stratégie visant à prévenir ou à atténuer le problème. Conformément, le but de cette étude est d'évaluer la performance et l'efficacité de diverses mesures d'atténuation de la liquéfaction des sols et des glissements de terrain. Les mesures d'atténuation envisagées ici comprennent: les colonnes de pierres (SC), les micro-pieux (MP), la densification (DS), les colonnes de pierres enrobées (ESC), l'injection de sol (GT) et l'abaissement des eaux souterraines (GL), qui sont couramment adoptées dans pratique de l'ingénierie. La performance et l'efficacité des mesures d'atténuation sont évaluées numériquement en termes de leurs réponses à la génération de pression interstitielle excessive dans le sol ainsi qu'à la déformation latérale des dépôts de sol due à l'excitation du mouvement sismique. Les résultats indiquent généralement que les options SC, ESC et DS sont plus efficaces pour empêcher la génération d'une pression interstitielle excessive, et donc pour réduire la liquéfaction du sol, que les autres options. Nous remarquons également que les options MP, SC et ESC seraient plus efficaces pour prévenir la déformation latérale, et donc pour éviter le glissement ou la propagation latérale dans les dépôts de sol.

Keywords: Mitigation measures; liquefaction flowslide; sloping ground; numerical assessment.

1 INTRODUCTION

Soil liquefaction is the phenomenon associated with strong earthquake which would be of the most catastrophic consequences of earthquake and thus has caused severe damage to the structures. Mainly, liquefaction induced earthquake might cause a significant loss of strength of soil masses with a progressive generation of pore pressure, and thus resulting in large permanent deformation, including

lateral spreading and settlement), and even flowslide failure of soils. Case histories were observed as the Petobo flow failure causing significant movement in a mildly sloping ground due to 2018 Palu-Donggala Indonesia earthquake (Kusumawardani, et al., 2021). Consequently, one of the most important strategy of earthquake-resistant design is to avoid or decrease liquefaction-induced deformations of foundation soils. Ground improvement and soil reinforcement are the most useful methods for improving the strength properties of soils and have been performed in order to avoid or decrease the liquefaction-induced soil deformations and associated damage. For example, the geosynthetics are main materials used for increasing the strength and stability of geotechnical structures (Hosseinpour et al., 2010). Several liquefaction mitigation techniques have been proposed over the years, including densification, grouting, and groundwater lowering. Although, the majority of these methods proves inapplicable or difficult to implement for various reasons and has been based on conceptual understanding or simplified analysis. Accordingly, the mitigation of liquefaction disasters would be a primary concern in engineering practice. Through rigorous finite element analyses, this paper addresses assessment of several liquefaction mitigation measures, including stone-column (SC), micro-pile (MP), densification (DS), encased stone column (ESC), soil grouting (GT), and groundwater lowering (GL), with an aim to provide a clearer understanding on effectiveness of ground improvement methods and to assess the liquefaction-induced soil deformations to acceptable levels for construction.

2 ANALYSIS METHOD

The assessment adopts a numerical tool for all simulations by using OpenSeesPL, which is a graphical user interface for conducting 3D ground-structure finite element analysis (http://opensees.berkeley.edu). A 20-8-node element is assumed, where 20 nodes are for solid translation degree for freedom and 8 corner nodes for fluid pressure. Multi-yield conical surfaces with considering phase transformation are applied for soils. The couple solid-fluid option of the software enables the performance of liquefaction studies. We describe the results of 3D seismic response with considering the behavior of soil in the center and the edge of soil column. In total, 88 simulations were performed to explore different combinations of influence factors, including the original cases (i.e., without any improvement).

Figure 1 indicates a typical soil column of the improved ground with a depth of 30 m, where a periodic boundary condition is assumed for the vertical faces and fix end at the base of column. Due to symmetric, only one half of the soil column is assumed in the numerical analysis. As indicated, the seismic shaking is assigned at the base of the soil column and acting in x-direction.

A liquefaction-prone area at Chuoshui river alluvial fan-delta (CRAFD; Chang et al., 2012) is selected as the target site with a groundwater level of 3.84 m below ground surface, where the log of Borehole W5-3, as shown in Figure 2, is adopted as the soil deposit with improvements by several mitigation measures in current study. It is noticed that the numerical analyses composed of clay and silt layers beneath a deposit of very loose sand to medium which are prone to liquefaction due to seismic shaking. Tables 1 and 2 indicate the assumed material parameters of soil deposit and mitigation as well as geosynthetic measures in numerical simulations.

The input motion of this study adopts the recorded motion at CHY002 station during 1999 Chi-Chi earthquake (M_W = 7.6) of Taiwan. The recorded motion, however, should be scaled to the design earthquake of the site (M_W = 7.1 and a_{max} = 0.308g) based on local building code (MOI, 2011), and then deconvoluted from ground surface to a depth of 30m of the site for OpenSeesPL analysis. Figure 3 shows the deconvoluted input motion for this study (a_{max} = 0.250g).

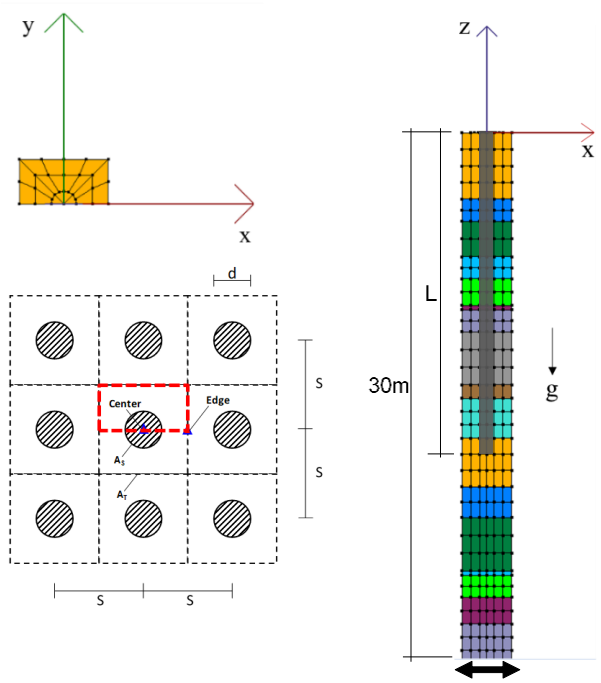

Figure 1. Finite element meshes of representative soil column for numerical simulations.

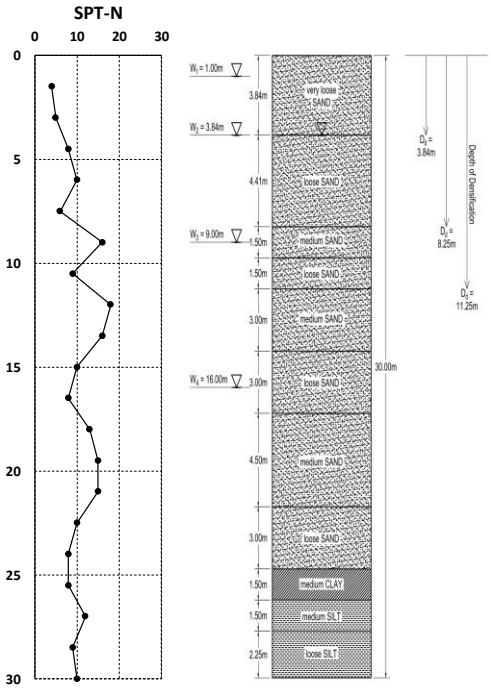

Figure 2. Typical soil/SPT-N profile, based on Borehole W5-3 in CRAFD, for current analysis.

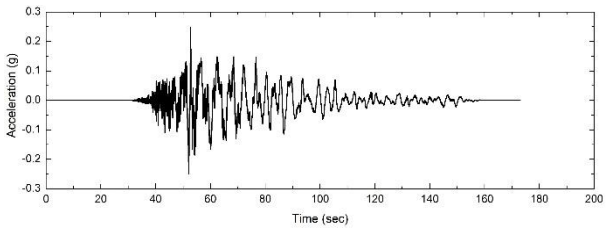

Figure 3. Deconvoluted input motion originally recorded at Station CHY002 (ground surface), in proximity of Borehole W5-3 with a distance < 2 km, during the 1999 Chi-Chi earthquake of Taiwan.

3 ASSESSMENT RESULTS

A comparative study of the seismic performance evaluation of stone-column (SC), micro-pile (MP), densification (DS), encased stone column (ESC), soil grouting (GT), groundwater lowering (GL) is compared with the original deposit (i.e., original ground, OG; without improvement). Typical range of design specifications for each of the options are selected, as indicated in the relevant figures, with varied spacing (s) for SC options, embedment depths (L) for MP options, depth of densification (D_d), thickness of geosynthetic (t) for ESC option, ground improvement ratio (Ir) for GT option, depth of groundwater (W) for GW option.

Table 2. Geosynthetic parameters.

Parameter	Geosynthetic	References
γ_{geosyn}(t/m^3)	0.13	IndoFelt Specification
v_{geosyn}	0.30	Murugesan and Rajagopal, 2006
E (kN/m^2)	1.00×10^6	Tang et al., 2015
k_{geosyn} (m/s)	1.00×10^{-3}	Tang et al., 2015
J (kN/m)	1.00×10^3	Tang et al., 2015
GJ (kN/m^2)	3.85×10^8	For t= 1mm, E= 10^6 kPa
k_{SC} (m/s)	1.00×10^{-2}	
G (kN/m^2)	3.85×10^5	
B (kN/m^2)	8.33×10^5	

Note: γ_{geosyn} = unit weight; v_{geosyn} = Poisson's ratio; E = Young's modulus; k_{geosyn} = permeability of geosynthetic; J = stiffness of geosynthetic; GJ = torsional rigidity; k_{SC} = permeability of stone-column; G = shear modulus of geosynthetic; B = bulk modulus of geosynthetic; Rayleigh damping for geosynthetic is 2%.

3.1 Excess pore pressure generation

For level ground, the computed excess pore pressure at a depth of 7m of deposit are shown in Figure 4. As seen, the SC, ESC, and DS options are more effective in dissipating the excess pore pressure than the other

Table 1. Adopted material parameters for original soil deposit (original ground; OG) and for liquefaction mitigation options of stone-column (SC) and micro-pile (MP).

Parameters	Original Ground (OG)						Stone Column (SC)	Micro Pile (MP)
	Very Loose SAND	Loose SAND	Medium SAND	Loose SILT	Medium SILT	Medium CLAY		
γ (kN/m^3)	16.7	16.7	18.6	16.7	18.6	14.7	18.5	24.5
ϕ (deg.)	29	29	33	29	33	0	33	-
c (kPa)	-	-	-	-	-	37	-	-
ϕ_{PT} (deg.)	29	29	27	29	27	-	27	-
G_r (kPa)	5.5E4	5.5E4	7.5E4	5.5E4	7.5E4	6.0E4	7.5E4	1.4E7
B_r (kPa)	1.5E5	1.5E5	2.0E5	1.5E5	2.0E5	3.0E5	2.0E5	-
K_{soil} (m/s)	6.6E-5	6.6E-5	6.6E-5	1.0E-7	1.0E-7	1.0E-9	-	-
K_{SC} (m/s)	-	-	-	-	-	-	1E-4, 1E-2, 1E0	-
E_r (kPa)	-	-	-	-	-	-	-	3.5E7
ν	-	-	-	-	-	-	-	0.2
σ_{py} (kPa)	-	-	-	-	-	-	-	5.2E4

Note: γ = unit weight; ϕ = friction angle; c = cohesion; ϕ_{PT} = phase transformation friction angle; G_r = shear modulus at a reference effective confining pressure of 80kPa; B_r = bulk modulus at a reference effective confining pressure of 80kPa; K_{soil} = hydraulic conductivity of soil; K_{SC} = hydraulic conductivity of stone-column; E_r = Young's modulus at a reference effective confining pressure of 80kPa; ν = Poisson's ratio; σ_{py} = yield stress.

options. The GT option shows decreasing in excess pore pressure and indicates no soil liquefaction at this depth. The results of excess pore pressure for GL option would be zero. Due to the soil-structure interaction, the excess pore pressure response in soil is oscillating severely by shaking for the MP option.

3.2 Lateral deformation time history

Figure 5 shows lateral deformation time histories computed at the depth of 7m of a mildly sloping ground (i=3deg.). As seen, the MP, SC, and ESC options would be more effective in preventing the lateral deformation than the other options, it is due to the increasing of the stiffness of soil mass. The GT and DS options would increase their inertia and lateral deformations are close or even more than the case of the original ground (OG).

3.3 Lateral deformation profile

Figure 6 shows the lateral deformation profiles of soil deposit with a slightly inclined ground (i=3deg.). Obviously, the MP, SC, and ESC options are most effective in preventing the lateral movement of soil deposits than the other options. The GL option would reduce the lateral movement by lowering the groundwater level down to 9m, however, not as effective as the MP, SC, and ESC options. The DS and GT options would densify or solidify the ground and reduce to some degree the generation of excess pore pressure, however, they tend to amplify the lateral movement as a result of the increase of soil density and inertia force by the shaking.

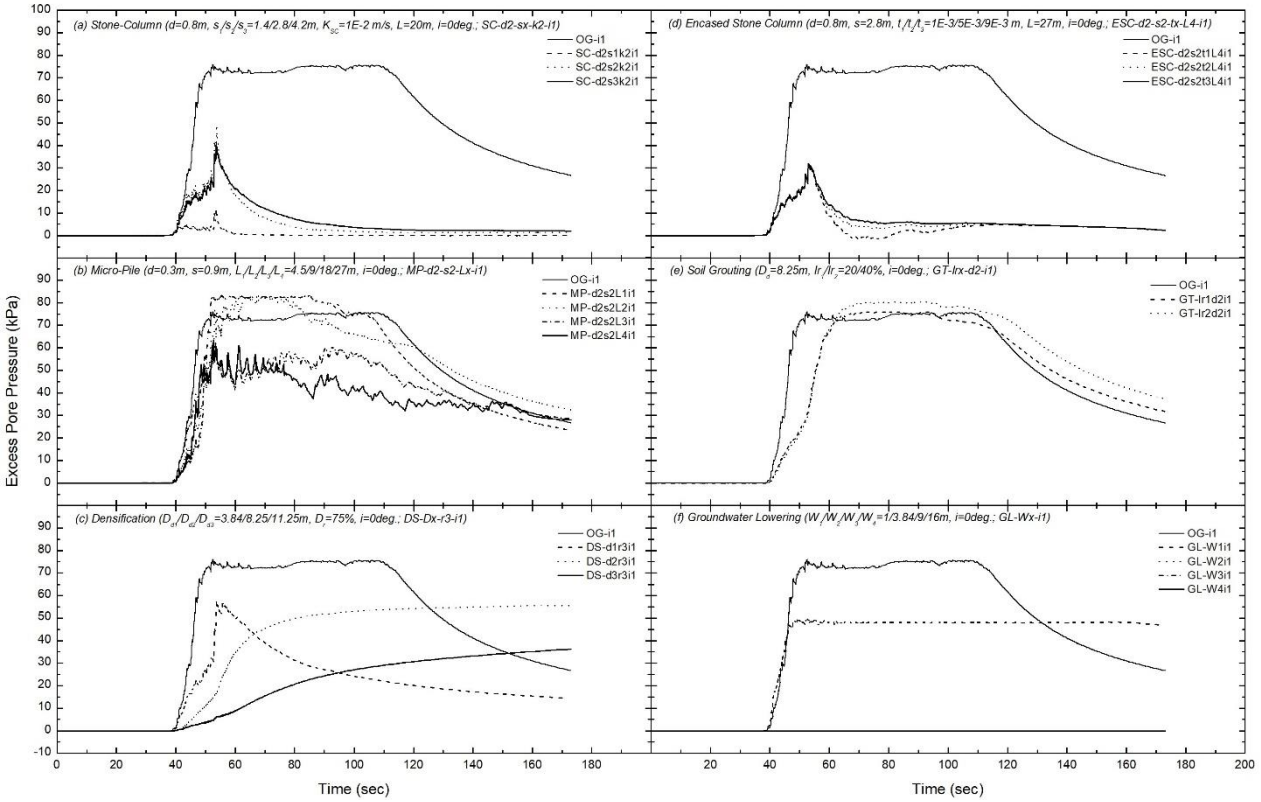

Figure 4. Computed excess pore pressure time histories at a depth of 7m (loose SAND) of the level ground (i=i_1=0deg.) for various liquefaction mitigation options. *(Note: OG – original ground; SC – stone-column; MP – micro-pile; DS – densification; ESC – encased stone column; GT – soil grouting; GL – groundwater lowering).*

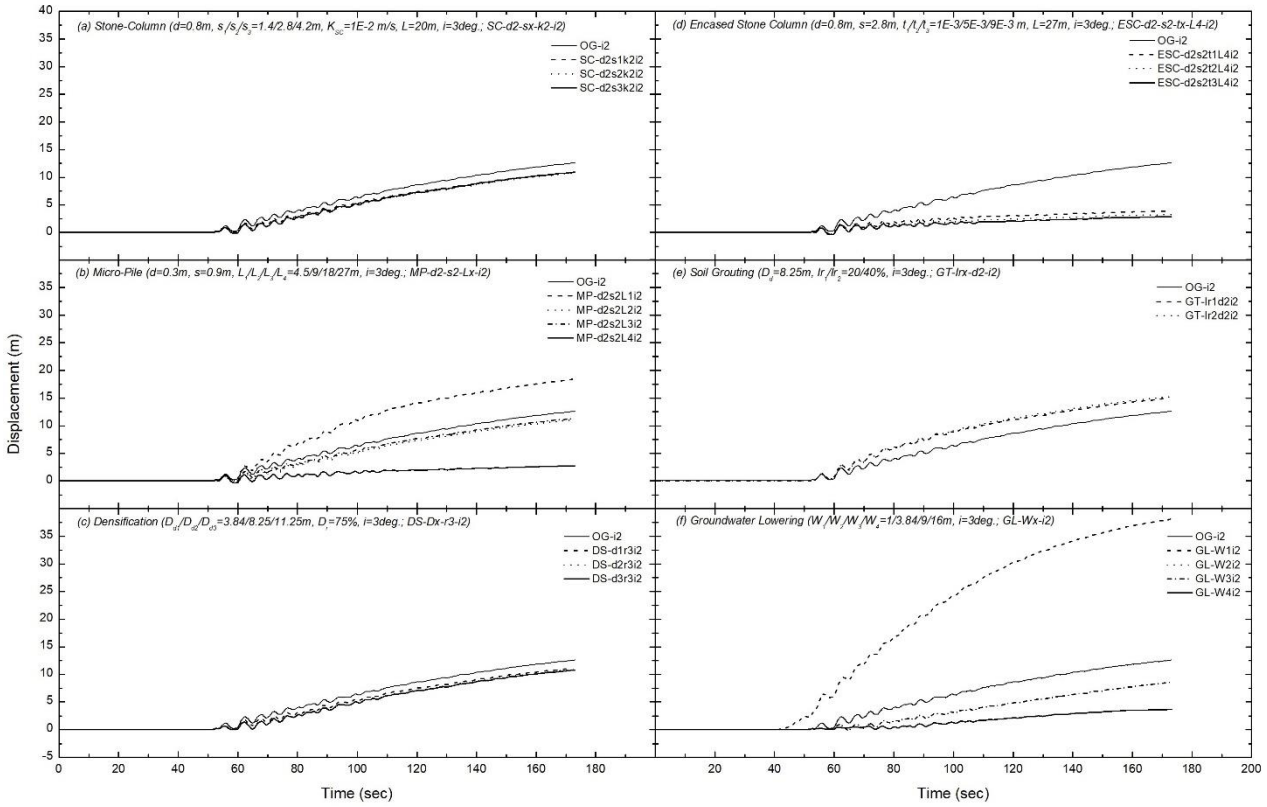

Figure 5. Computed lateral deformation time histories at a depth of 7m (loose SAND) of the inclined ground ($i=i_2$=deg.) for various liquefaction mitigation options. (Note: OG – original ground; SC – stone-column; MP – micro-pile; DS – densification; ESC – encased stone column; GT – soil grouting; GL – groundwater lowering).

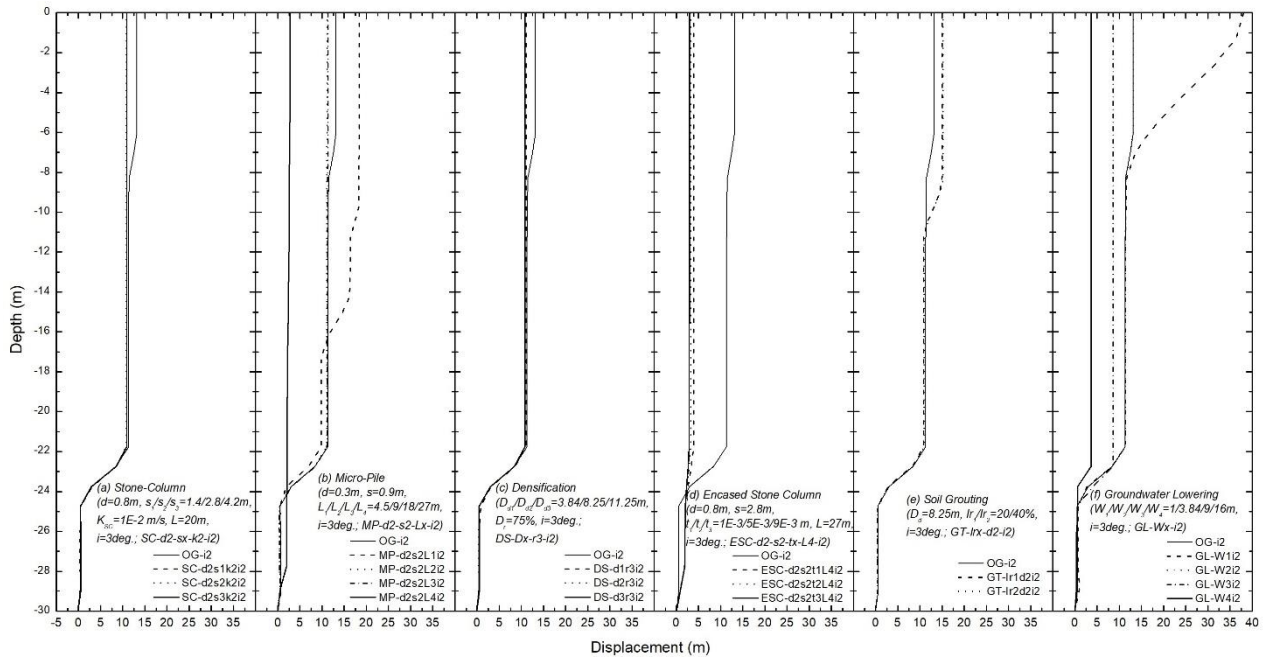

Figure 6. Computed lateral deformation profiles of an inclined ground ($i=i_2$=3deg.) for various liquefaction mitigation options. (Note: OG – original ground; SC – stone-column; MP – micro-pile; DS – densification; ESC – encased stone column; GT – soil grouting; GL – groundwater lowering).

4 CONCLUSIONS

Through a comprehensive numerical assessment of various liquefaction mitigation options, including stone-column (SC), micro-pile (MP), densification (DS), encased stone column (ESC) soil grouting (GT), and groundwater lowering (GL). Some key points and findings of the study are summarized as follows:

- The SC, ESC, and DS options are more effective in dissipating the excess pore pressure than the other options through drainage pathways and increased soil density. The ESC option would be improved soil stability by reinforcing the soil. The encasement provides additional lateral confinement to the stone column, facilitating efficient dissipation of excess pore pressure and enhancing soil stability.
- The GT and GL options would slightly reduce pore water pressure within the soil through soil densification and water table control, respectively. These options contribute to increased soil stability and decreased susceptibility to ground failure during seismic shaking.
- The MP, ESC, DS, and GT options are most effective in preventing the lateral deformation of soil deposits than the other options. They tend to increase the soil density, stiffness, and inertia force by shaking, thereby enhancing stability. The MP option would tend to amplify the lateral movement if the embedment depth is less than the liquefiable layers. The GT and GL options would tend to indirectly influence lateral deformation by stabilizing soil properties, though their direct impact on lateral displacement may vary.

REFERENCES

Chang, M., Kuo, C. P., Hsu, R. E., Shau, S. H. and Lin, T. M. (2012). Liquefaction potential and post-liquefaction settlement evaluations of Chuoshui River Allluvial Fan in Taiwan. *Bulletin of Engineering Geology and the Environment*, 7: 325-336. http://doi.org.10.1007/s10064-011-0390-7.

Hosseinpour, I., Mirmoradi, S. H., Barari, A. and Omidvar, M. (2010). Numerical evaluation of sample size effect on the stress–strain behavior of geotextile-reinforced sand. *Journal of Zhejiang University-Science A*, 11(8): 555–562. http://doi.org.10.1631/jzus.A0900535.

Kusumawardani, R., Chang, M., Upomo, T. C., Huang, R. C., Fansuri, M. H. and Prayitno, G. A. (2021). Understanding of Petobo liquefaction flowslide by 2018.09.28 Palu-Donggala Indonesia earthquake based on site reconnaissance. *Landslides*, 18: 3163-3182. http://doi.org.10.1007/s10346-021-01700-x.

Ministry of the Interior (MOI). (2011). *Construction and Planning Agency, Taiwan. Seismic Resistance Design of Buildings - Code and Explanations* (in Chinese).

Murugesan, S. and Rajagopal, K. (2006). Geosynthetic-encased stone column: Numerical evaluation. *Geotextiles and Geomembranes*, 24(6): 349-358. http://doi.org.10.1016/j.geotexmem.2006.05.001.

Tang, L., Cong, S., Ling. X., Lu, J. and Elgamal, A. (2015). Numerical study on ground improvement for liquefaction mitigation using stone columns encased with geosynthetics. *Geotextile and Geomembrane*, 43(2): 190-195. http://dx.doi.org/10.1016/j.geotexmem.2014.11.011.